

A Grid-based Method for Removing Overlaps of Dimensionality Reduction Scatterplot Layouts

Gladys M. Hilasaca, Wilson E. Marcílio-Jr, Danilo M. Eler, Rafael M. Martins, and Fernando V. Paulovich, *Member, IEEE*

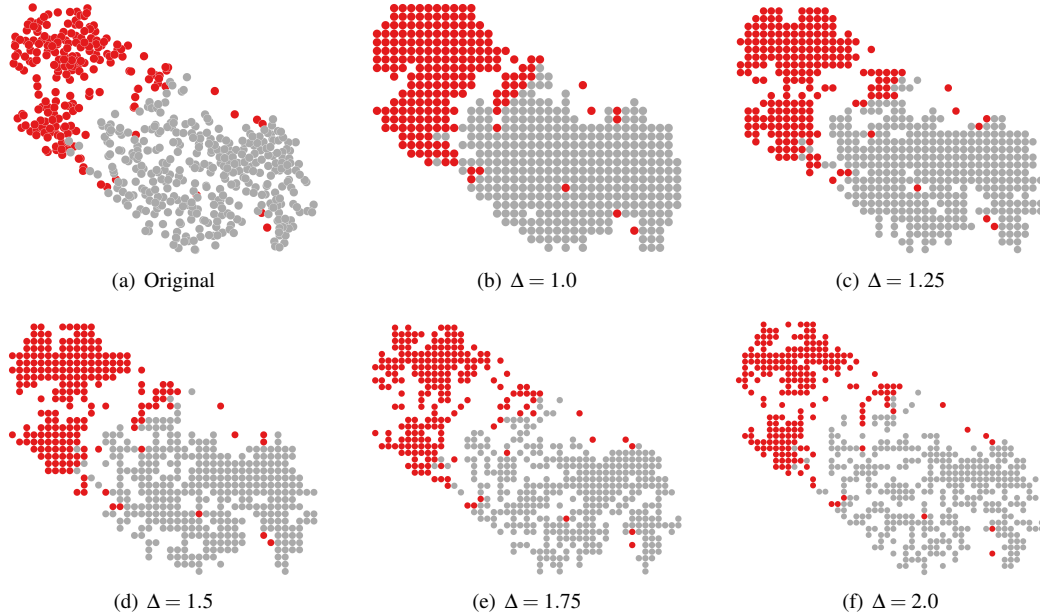


Fig. 1. Overlap removal varying the space allocated for the visual representation (or reducing glyphs' size). Given that red points are rendered before gray points, some are occluded due to overplotting (a). After applying DGrid, such points become visible, but the frontiers between groups and sub-groups are lost (b). As the visual area is increased (c-f), multiplying it by a factor (Δ), the original appearance of (sub)group separation is recovered, resulting in a readable overlap-free layout.

Abstract—Dimensionality Reduction (DR) scatterplot layouts have become a ubiquitous visualization tool for analyzing multidimensional datasets. Despite their popularity, such scatterplots suffer from occlusion, especially when informative glyphs are used to represent data instances, potentially obfuscating critical information for the analysis under execution. Different strategies have been devised to address this issue, either producing overlap-free layouts which lack the powerful capabilities of contemporary DR techniques in uncovering interesting data patterns, or eliminating overlaps as a post-processing strategy. Despite the good results of post-processing techniques, most of the best methods typically expand or distort the scatterplot area, thus reducing glyphs' size (sometimes) to unreadable dimensions, defeating the purpose of removing overlaps. This paper presents *Distance Grid (DGrid)*, a novel post-processing strategy to remove overlaps from DR layouts that faithfully preserves the original layout's characteristics and bounds the minimum glyph sizes. We show that DGrid surpasses the state-of-the-art in overlap removal (through an extensive comparative evaluation considering multiple different metrics) while also being 2 or 3 orders of magnitude faster for large datasets.

Index Terms—Dimensionality reduction, Multidimensional Projection, Scatterplots, Overlap removal

1 INTRODUCTION

Scatterplots are among the most prevalent visualizations in exploratory data analysis [40, 52, 63]. Despite their popularity, they suffer from

- *G.M. Hilasaca is with University of São Paulo. E-mail: marlenyh@icmc.usp.br*
- *W.E. Marcílio-Jr and D.M. Eler are with São Paulo State University. E-mail: wilson.marcilio@unesp.br, danilo.eler@unesp.br*
- *R. M. Martins is with Linnaeus University. E-mail: rafael.martins@lnu.se*
- *F.V. Paulovich is with Eindhoven University of Technology. E-mail: f.paulovich@tue.nl*

Manuscript received xx xxx. 201x; accepted xx xxx. 201x. Date of Publication xx xxx. 201x; date of current version xx xxx. 201x. For information on obtaining reprints of this article, please send e-mail to: reprints@ieee.org. Digital Object Identifier: xx.xxx/TVCG.201x.xxxxxx

the same issue present in most 3D (we love to hate) visual representations: *occlusion* [5]. As the overlap between visual markers (or glyphs) representing the data instances increases, scatterplots become less effective [52, 53, 63], affecting our comprehension [34] and the correctness of analytical tasks, since non-visible objects are prone to be ignored [17]. Even simple design choices like the glyphs' rendering order [40] can result in misleading layouts, and the problem is amplified when they convey complex information that occupies more space, such as images [16] or other informative glyphs [8].

Different strategies have been proposed for the general case to tackle this problem, including sampling, abstraction, re-sizing, changing opacity, and a combination of those [63]. Despite their differences, the underlying common idea is to transform a scatterplot so that typical tasks of correlation estimation, class separation, outlier detection, distribution detection, and point value reading [40] are still valid. For the particular case of Dimensionality Reduction (DR) visualization [45],

this list can be relaxed. Since exact positions in the axes are usually unimportant, especially when non-linear techniques are used, correlation estimation and point-value reading are irrelevant. This allows some flexibility in the glyphs' positions which can be taken advantage of during overlap removal.

Some solutions to address this problem can be found in the literature, usually split into overlap-free and overlap-removal strategies. In the former group, techniques seek to create DR scatterplots without overlap [46, 47] but lack the powerful capabilities of contemporary DR techniques in uncovering interesting data patterns. On the latter, post-processing strategies are devised to remove overlaps of any given scatterplot by rearranging the glyphs while maintaining, as much as possible, the characteristics of the original scatterplot. In this group, optimization of cost functions has been suggested [21, 24], with the inherent problems of numerical stability of such solutions. Triangulation [44] and orthogonal scan-line-based algorithms are also common [15, 22, 25, 42], usually delivering better results. In general, however, existing solutions still have problems preserving multiple scatterplot characteristics such as plot dimensions and the glyphs' relative positions, favoring some aspects to the detriment of others and often producing results with glyphs of unreadable dimensions, defeating the purposes of overlap removal.

This paper presents *Distance Grid (DGrid)*, a novel approach for overlap removal in DR scatterplots. It combines a density-based strategy to generate auxiliary points with a novel space-partitioning method to produce overlap-free layouts that faithfully preserve different characteristics of input scatterplots. Compared to seven state-of-the-art techniques, DGrid presents the best trade-off regarding multiple aspects while producing low distortions and bounding the dimensions of the created layouts, consistently resulting in visual representations with readable glyphs. Also, in a user study with 42 participants, DGrid was selected as the best technique for preserving the general appearance of original scatterplots while rendering aesthetically pleasant layouts.

In summary, the main contributions of this paper are:

- A novel, fast, and highly precise method for overlap removal in DR scatterplots that presents a good trade-off between different aspects of layout preservation;
- A thorough analysis of the literature to better formalize the problem of scatterplot characteristics' preservation for overlap removal, consolidating a set of concepts and metrics;
- An extensive comparative analysis of overlap removal techniques involving seven state-of-the-art approaches plus our proposed technique.
- The results of a comprehensive user study that identified the preferences of 42 users regarding aesthetics, accuracy, and ease of interpretation, over the same set of seven approaches plus DGrid.

The remainder of this paper is divided as follows. Sec. 2 discusses the differences between scatterplot overlap removal and sampling concepts and examines the related work. Sec 3 formalizes the overlap removal problem, consolidates the existing metrics, and presents our method. Sec 4 presents a comprehensive analysis, comparing DGrid with the state-of-the-art, discusses potential use cases, and finishes with a user study. Finally, Sec. 5 discusses the existing limitations and Sec. 6 draws our conclusions.

2 RELATED WORK

Occlusion in scatterplots is a well-known problem [5] that can make such a popular visual representation less effective [52, 53, 63]. In the literature, different solutions are presented to address the involved issues, usually *transforming visual markers or glyphs*, for instance, (i) by adjusting their transparency [41], sizes [30, 31] or using density and contour plots [9, 35, 56], (ii) by carefully *sampling* the glyphs to display [4, 12], or (iii) by re-arranging glyphs' positions to *remove overlaps*. Here we refrain from discussing the existing literature on glyphs' transformation and sampling since, although relevant solutions to improve the visual aspect of scatterplots, they do not solve the problem of removing overlaps, the focus of this paper.

In general, when scatterplots are used to represent Dimensionality Reduction (DR) layouts, the two most common strategies to address occlusion while maintaining all glyphs are: (1) creating overlap-free layouts from scratch; or (2) eliminating overlaps as a post-processing strategy. Some techniques have been proposed in the former group, such as IncBoard [47] and HexBoard [46]. Although interesting solutions, they lack the powerful capabilities of contemporary DR techniques to uncover meaningful data patterns. In the latter (i.e. post-processing strategies), some methods remove overlaps by mapping scatterplot points into orthogonal grid cells preserving distances, such as IsoMatch [19], Kernelized Sorting [48], and NMAP [14]. However, grid approaches negatively affect important analytical tasks such as class separation, outlier, and distribution detection [40], since the empty space is removed and gaps are usually beneficial [39]. It is also possible to create distance-preserving grids without considering DR layouts as inputs [2, 18, 37, 49, 55, 58, 61], but they are out of our scope.

Still regarding post-processing strategies, a group of techniques heuristically rearrange layouts by moving glyphs while maintaining, as much as possible, the characteristics of a given scatterplot [10, 33]. This paper discusses the problem when the visual area assigned to render a glyph is rectangular (a bounding box). We refrain from discussing other potential shapes, for instance, diamonds [38], since comparison among techniques would be impractical once the shape is considered when calculating most layouts' quality metrics (later discussed in Sec. 3.1).

RWordle [54] is one example of overlap-removal technique that uses bounding boxes. It positions glyphs by searching for empty positions using a spiral pattern, with two variants that differ in the order the points are processed: RWordle-L orders glyphs along a scan-line, while RWordle-C orders them using distances. RWordle is not precise in preserving essential characteristics of the original layout, such as the similarity relationships among glyphs [33]. It also results in unreasonable running time for dense scatterplots, causing excessive displacement of glyphs and loss of distance relations.

ProjSnippet [24] focuses specifically on distance preservation by maximizing an energy function that accounts for similarity preservation and overlap removal. It has limitations when the original scatterplot has groups of points with high-density. In these cases, the technique uses too much space to reduce overlap, often distorting and creating overlap-free layouts with unreadable (tiny) glyphs, defeating the purpose of removing overlaps. One further problem with ProjSnippet is the optimization procedure that sometimes suffers from numerical instability. Another technique, called MIOLA [23], uses mixed-integer quadratic programming to rearrange rectangular boxes in the visual space. MIOLA usually presents more compact layouts after overlap removal. However, it does not preserve well orthogonal ordering and neighborhoods [23].

Another technique that relies on optimization is PRISM [21]. PRISM creates a proximity graph on top of the original layout using triangulation, then minimizes a stress function considering an overlap factor between each pair of nodes in the graph. Scatterplot density also affects its running time, and it suffers from similar problems with optimization instability, sometimes resulting in layouts that are not overlap-free. Triangulation is also used in the GTree method [44], with the triangulation edges used to define a cost function that builds a minimum cost spanning tree. GTree interactively grows the edges' length of such tree until there are no more overlaps. It maintains the original scatterplot aspect-ratio but moves glyphs excessively, requiring too much space for the final layout and considerably reducing glyphs size [10].

A well-explored strategy to reduce overlap is to process the x and y axes individually. The Push Force-Scan (PFS) [42] is one of the pioneers. PFS orders rectangles in the horizontal/vertical direction and applies the minimum movement to remove overlap among subsequent glyphs, focusing on orthogonal ordering preservation. PFS tends to displace glyphs considerably, not preserving the initial layout's aspect-ratio [10], and adds unnecessary spaces between glyphs. To reduce such spaces, PFS' [25] moves glyphs horizontally/vertically based on the maximum movement distance from previous glyphs, unlike the sum of previous ones as PFS. The overlap-free layout is improved, but it still presents unnecessary spread and may not maintain the input

layout’s aspect-ratio. Another technique that treats each axis separately is VPSC [15]. It defines non-overlap constraints for the x and y axes related to how much a glyph needs to be moved in the corresponding direction. As the previous techniques, the resulting layouts diverge from the original layouts for scatterplots presenting dense groups of points.

Finally, ReArrange [22] considers pairs of overlapping nodes, one by one, resolving the occlusion problem with the smallest displacement possible while preserving orthogonal order. Similar to VPSC, ReArrange finds overlaps among glyphs using a line-sweep algorithm and applies overlap removal on x and y axes separately. ReArrange is one of the best-performing approaches, but it distorts the original layout’s aspect-ratio and increases the layout dimensions, reducing glyphs sizes.

In our technique, aspect-ratio preservation and spread are explicitly controlled, producing overlap-free layouts with low distortions and the same dimensions as the original layouts, or with a controlled upper-bound, resulting in visualizations with readable glyphs (assuming they are legible on the original scatterplot). Also, distance and neighborhood relationships are precisely maintained, an essential aspect in many DR analytical tasks, without negatively affecting running time.

3 METHOD

Before discussing our solution, we first formalize the problem of overlap removal in scatterplots and consolidate the existing literature about quality metrics.

3.1 Problem Formulation and Principles

In general terms, given a scatterplot \mathcal{P} composed of N points or glyphs $\mathcal{P} = \{p_1, \dots, p_N\} \in \mathbb{R}^2$, where (w_i, h_i) are the dimensions of the bounding box around p_i and (x_i, y_i) are the top-left corner coordinates of such bounding box, *overlap removal* techniques aim to create a new scatterplot $\mathcal{P}' = \{p'_1, \dots, p'_N\} \in \mathbb{R}^2$ where the glyphs’ superposition are removed and the overall structure of \mathcal{P} is preserved as much as possible. The quality of overlap-free layouts can be defined and measured through a set of different, often conflicting principles and metrics. Following, we present a consolidated list of the most important principles and associated metrics found in the literature, which later are used to evaluate and compare our solution with the state-of-the-art.

P1 – Remove glyphs’ overlaps. The resulting scatterplot \mathcal{P}' should present minimum overlap among glyphs, eliminating occlusions that may hide important information. To measure occlusion, we average the pairwise *overlap coefficient* [50] among all graphical glyphs, computing

$$overlap = \sqrt{\frac{1}{N(N-1)} \sum_i \sum_{j \neq i} \frac{\mathcal{A}(p_i \cap p_j)}{\min\{\mathcal{A}(p_i), \mathcal{A}(p_j)\}}}, \quad (1)$$

where $\mathcal{A}(p_i)$ denotes the bounding box area around p_i , and the operator \cap returns the intersection of two glyphs. The overlap coefficient ranges in $[0, 1]$ with 0 indicating an overlap-free layout.

P2 – Preserve glyphs’ global and local distances. Given the typical application of DR layouts for interpreting distance and neighborhood relationships, the overlap-free layout \mathcal{P}' should preserve as much as possible the global distances between glyphs and local neighborhoods presented in the original scatterplot \mathcal{P} . To measure global preservation, we use the well-known *stress* [29], given by

$$stress = \sqrt{\frac{\sum_i \sum_j (||p_i - p_j|| - ||p'_i - p'_j||)^2}{\sum_i ||p_i - p_j||^2}}. \quad (2)$$

Stress ranges in $[0, +\infty]$ with 0 indicating perfect preservation of distances. Notice that to reduce distortions, the transformed layout \mathcal{P}' should be scaled to the same dimensions of the original layout \mathcal{P} . To measure the local neighborhood preservation, we use the usual *trustworthiness* [59], given by

$$trustworthiness = 1 - \frac{2}{NK(2N - 3K - 1)} \sum_i \sum_{j \in U_K^i} (r(i, j) - K), \quad (3)$$

where U_K^i is the set of points that are in the neighborhood of size K of $p'_i \in \mathcal{P}'$ but not in neighborhood of size K of $p_i \in \mathcal{P}$, and $r(i, j)$ is the rank of points p_j in the ordering according to the distance from p_i in the original scatterplot. Trustworthiness ranges in $[0, 1]$, the larger the better, and measures how different is the neighborhood rank of $p'_i \in \mathcal{P}'$ compared to the original neighborhood rank of $p_i \in \mathcal{P}$.

P3 – Preserve glyphs’ relative positions. An overlap-free layout \mathcal{P}' should not only preserve distances but also relative positions among glyphs. That is, if p_i is at left/right above/below of p_j , the same ordering should be observed in p'_i and p'_j . This is usually referred to as user mental map preservation and is measured using *orthogonal ordering* [43], given by

$$ordering = \frac{1}{N(N-1)} \left(\sum_{i,j} \begin{cases} 1, & \text{if } x_i > x_j \wedge x'_i < x'_j + \\ 0, & \text{otherwise} \end{cases} + \sum_{i,j} \begin{cases} 1, & \text{if } y_i > y_j \wedge y'_i < y'_j \\ 0, & \text{otherwise} \end{cases} \right). \quad (4)$$

The orthogonal ordering ranges in $[0, 1]$, with 0 indicating perfect order preservation.

P4 – Preserve aspect ratio. The overlap-free representation should preserve the original scatterplot’s aspect ratio, reducing distortions. The usual metric to estimate *aspect-ratio* [11] is

$$aspect = \max \left(\frac{W'_{bb} \times H_{bb}}{H'_{bb} \times W_{bb}}, \frac{H'_{bb} \times W_{bb}}{W'_{bb} \times H_{bb}} \right), \quad (5)$$

where W'_{bb} and H'_{bb} are the width and height of \mathcal{P}' bounding box, calculated using

$$\begin{aligned} W_{bb} &= |\max_{i \leq N} (x_i + w_i) - \min_{j \leq N} x_j| \\ H_{bb} &= |\max_{i \leq N} (y_i + h_i) - \min_{j \leq N} y_j| \end{aligned} \quad (6)$$

The *aspect ratio* ranges in $[1, +\infty]$, with 1 the target value.

P5 – Minimize glyphs’ displacement. The translations applied to the glyphs to remove the overlaps and create \mathcal{P}' should be as small as possible to preserve the general appearance of \mathcal{P} [43]. To measure this, we use the average displacement [60], given by

$$displacement = \frac{1}{N \sqrt{W'_{bb} * H'_{bb}}} \sum_i ||p_i - p'_i||. \quad (7)$$

The *displacement* ranges in $[0, 1]$, with 0 indicating no changes in glyphs’ positions. Notice that the center of both \mathcal{P} and \mathcal{P}' should be translated to the origin to better capture the relative movement [11].

P6 – Limit glyphs’ minimum size. Finally, the area occupied by the overlap-free representation should be limited to controlling glyphs’ minimum size, avoiding creating unreadable layouts and resulting in large empty areas [11]. Visual representations with glyphs that cannot be read defeat the general purpose of increasing layouts’ readability by removing overlaps. To quantify this, *layout spread* [43] can be measured using

$$spread = \frac{W'_{bb} \times H'_{bb}}{W_{bb} \times H_{bb}}, \quad (8)$$

where W_{bb} and H_{bb} are the original scatterplot bonding box dimensions calculated using Eq. (6).

In summary, in addition to the general goal of removing overlaps (**P1**), these principles capture two conflicting perspectives, *structure preservation* (**P2**, **P3**, and **P4**) and *readability* (**P5** and **P6**). For instance, consider the trivial solution of uniformly scaling the original scatterplot \mathcal{P} by the minimum possible factor that results in an overlap-free layout [38]. That would result in optimum values for **P1** (remove overlaps), **P2** (distances/neighborhoods preservation), **P3** (orthogonal ordering), and **P4** (aspect-ratio preservation). However, it would typically present poor results for **P5** (displacement) and **P6** (minimum glyphs size) since, for relatively dense scatterplots, the scale factor can be quite large, resulting in substantial amounts of empty spaces and tiny unreadable glyphs.

3.2 Distance Grid (DGrid)

Aiming at finding a good compromise between these perspectives, we present *Distance Grid (DGrid)*, a new solution based on grid assignment to completely remove overlaps in scatterplot visual representations, producing readable layouts while preserving as much as possible, the original scatterplot structures.

DGrid has two major phases divided into different steps (see Fig. 2). In the first phase, an orthogonal grid \mathcal{G} is superimposed to the scatterplot area with cell sizes equal to the dimensions of the largest bounding box glyph in \mathcal{P} , and with the number of rows R and columns C defined by the original scatterplot dimensions (width and height) **A**. Then, in the second phase, each scatterplot point is assigned to the closest individual cell so that overlaps are removed. The assignment phase is composed of three different steps. Since usually, the number of cells ($R \times C$) is much larger than the number of scatterplot points N (we later discuss what happens when this does not hold), we first carefully add extra points, called “dummy” points, in low-density regions of the scatterplot to represent empty spaces **B**. Once the “dummy” points are added, the original and “dummy” points are assigned to individual grid cells using a grid assignment process that minimizes displacement **C** then the “dummy” points are removed **D**. The general idea is to use the “dummy” points to represent empty regions in the scatterplot, so that frontiers between groups and outliers are preserved. The result is a complete overlap-free layout (**P1**) since each point is assigned to an individual cell, displacing the points as little as possible (**P5**), thus preserving original distances (**P2**) and relative positions (**P3**) while also maintaining the scatterplot aspect-ratio (**P4**) and the original glyph sizes (**P6**). We start by explaining how to generate the orthogonal grid and the “dummy” points.

3.2.1 Generating the Grid and Adding Dummy Points

Generating the orthogonal grid \mathcal{G} is straightforward. To limit glyphs’ minimum sizes (**P6**), the cell dimensions are set to (w_{max}, h_{max}) where w_{max} and h_{max} are the maximum width and height among all glyphs bounding boxes. Also, to preserve the aspect-ratio (**P4**), \mathcal{G} width and height is defined to be the same of the original scatterplot \mathcal{P} , setting the number of columns of \mathcal{G} to $C = \lceil W_{bb}/w_{max} \rceil$ and the number of rows to $R = \lceil H_{bb}/h_{max} \rceil$. Although fulfilling **P4** and **P6**, this only works if the number of cells $R \times C$ is larger than or equal to the number of points N . If this is not the case, the result is occluded glyphs, violating **P1**. To address such situations, the grid’s dimensions can be increased by a percentage factor $\Delta \geq 1$, setting

$$\begin{aligned} C &= \lceil \sqrt{\Delta} \times W_{bb}/w_{max} \rceil, \text{ and} \\ R &= \lceil \sqrt{\Delta} \times H_{bb}/h_{max} \rceil. \end{aligned} \quad (9)$$

This preserves the aspect-ratio (**P4**) of the overlap-free layout and potentially improves other structure-preserving metrics (**P2** and **P3**). However, it reduces the glyphs’ size considering that the final visual representation has the same dimensions of the original scatterplot \mathcal{P} , possibly violating **P6** depending on how large Δ needs to be defined.

After creating the orthogonal grid, points are assigned to the “closest” grid cells in \mathcal{G} to remove the overlaps. Given the nature of the proposed

assignment strategy (later discussed in Sec. 3.2.2), if \mathcal{P} is assigned to \mathcal{G} as is, all the points would be grouped in the top-right corner of the final layout. Therefore, to represent empty spaces aiming at preserving the general appearance of the original scatterplot, that is, the existing groups, frontiers between groups, and outliers, “dummy” points are added to the list of points to assign to \mathcal{G} . The idea is to add the “dummy” points in low-density regions but close to original points p_i . In this way, glyphs’ displacement is reduced (**P5**) since the potential movement of original points is reduced. Also, the represented empty spaces focus on the characteristics of the existing groups of points as much as possible since they are close to or within those groups (borders).

In this process, we first define a list of candidate “dummy” points $\mathcal{D} = \{d_1, d_2, \dots\} \in \mathbb{R}^2$, generating a point per each cell $g_i \in \mathcal{G}$ not occupied by any original point. Since original points will occupy N cells, we select $(R \times C) - N$ points placed in low-density regions from this list. In other words, we remove N “dummy” points from the candidate list considering the scatterplot density. To calculate the region density of a point d_i , we first count the number of original points lying inside each cell, defining $\mathbf{G}_{R \times C}$, then we convolve a Gaussian kernel of size $M \times M$ with \mathbf{G} setting d_i to its center, where M is calculated as

$$M = \frac{W_{BB} \times H_{BB}}{\sum_i^N (w_i \times h_i)}, \quad (10)$$

and kernel’s $\sigma = (M - 1)/6$ (notice that M is rounded to the closest larger odd number). In this way, the kernel size is proportional to the level of details allowed in the overlap-free layout, which is proportional to the number of empty cells per occupied cell and smoothly covers the region. We also zero-padded \mathbf{G} adding $M/2$ rows and columns to its top/bottom and left/right, respectively.

Algorithm 1 Creating “dummy” points.

Input:

$\mathcal{P} = \{p_1, p_2, \dots, p_N\}$ ▷ Original Scatterplot
 W_{bb}, H_{BB} ▷ Bounding box of \mathcal{P} (Eq.(6))
 $\Delta \geq 1$ ▷ Visual space scaling factor. Increase empty space.
 w_{max}, h_{max} ▷ Max glyph bounding-box width/height in \mathcal{P}
 $x_{min}, x_{max}, y_{min}, y_{max}$ ▷ Max/min glyph coordinates in \mathcal{P}
 $C \leftarrow \lceil \sqrt{\Delta} \times W_{bb}/w_{max} \rceil$ ▷ Calculate the grid number of columns
 $R \leftarrow \lceil \sqrt{\Delta} \times H_{bb}/h_{max} \rceil$ ▷ Calculate the grid number of rows

Output:

$\mathcal{D} = \{d_1, \dots, d_{(R \times C) - N}\}$ ▷ “Dummy” points

function DUMMY(\mathcal{P}, C, R)

$\mathbf{G}_{R \times C} \leftarrow \text{COUNT}(\mathcal{P}, C, R)$ ▷ Count the number of points per cell
 $\mathbf{K}_{M \times M} \leftarrow \text{MASK}(\mathcal{P})$ ▷ Calculate an $M \times M$ kernel (Eq.(10))
for $r < R$ **do**
 $y \leftarrow r \times (y_{max} - y_{min}) / (R - 1) + y_{min}$
 for $c < C$ **do**
 if $g_{r,c} = 0$ **then** ▷ Grid cell is empty
 $x \leftarrow c \times (x_{max} - x_{min}) / (C - 1) + x_{min}$
 $\delta \leftarrow \sum_i^M \sum_j^M k_{i,j} \times g_{\lfloor r - (M/2) + j \rfloor, \lfloor c - (M/2) + i \rfloor}$
 $\mathcal{D} \leftarrow \mathcal{D} \cup (x, y, \delta)$ ▷ Add candidate “dummy” point
 end if
 end for
end for
return FILTER($\mathcal{D}, (R \times C) - N$)
end function

If different candidate “dummy” points present the same density and it is necessary to choose some of them for the final $(R \times C) - N$ list, we select the closest to any original point. Algorithm 1 details the process of creating the “dummy” points. In this algorithm, function COUNT(\mathcal{P}, C, R) returns a grid $\mathbf{G}_{R \times C}$ with the number of original points per grid cell, MASK(\mathcal{P}) return the Gaussian kernel of size $M \times M$, and FILTER($\mathcal{D}, (R \times C) - N$) return a list of $(R \times C) - N$ “dummy” points placed in low-density regions close to original points.

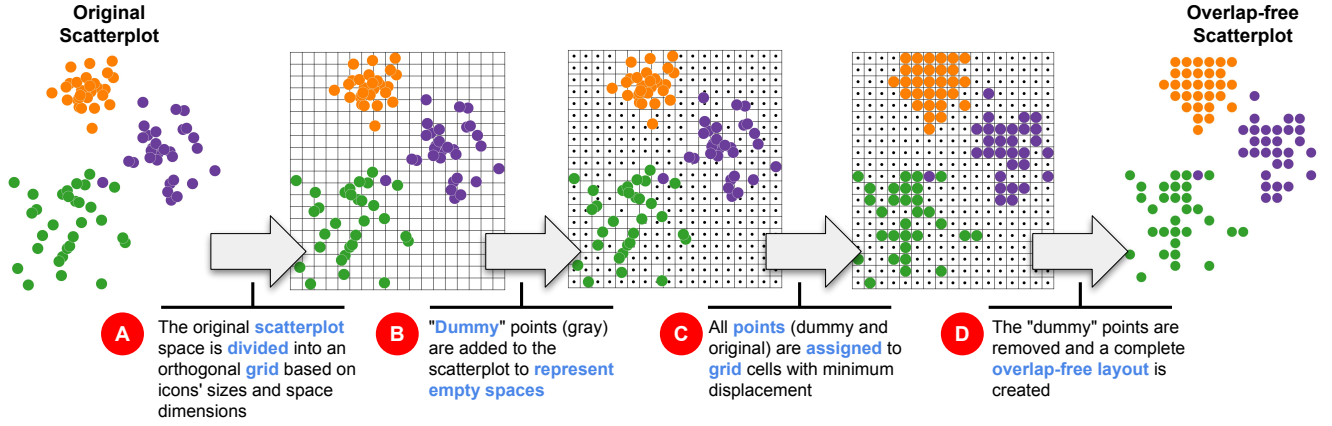


Fig. 2. Overview of DGrid process. The scatterplot area is first split into a grid (A), and “dummy” points (small black dots) are crafted to represent empty space (B). Finally, original and “dummy” points are assigned to grid cells (C), and the “dummy” points are removed (D), resulting in a completely overlap-free layout.

As already discussed, $R \times C \geq N$, in other words, $M \geq 1$ (Eq. (10)) so all points can be assigned to individual grid cells. Although satisfying this restriction guarantees that an overlap-free layout is produced, the results may degenerate if M is too close to 1. With $M \approx 1$, the number of grid cells is too close to the number of original points, so only a few “dummy” points are used to represent empty spaces, and the result is a layout without clear borders between groups and outliers. A simple solution is to increase Δ (see Eq. (9)), which can be interactively done since, in general, DGrid is very fast to execute.

3.2.2 Grid Assignment

The last step in our process is to assign each point $c_i \in \mathcal{C} = \mathcal{P} \cup \mathcal{D}$ (the complete set of original and “dummy” points) to an individual grid cell $g_i \in \mathcal{G}$ position, therefore completely removing the overlaps (P1). For a target grid \mathcal{G} of dimension (R, C) (rows and columns), this process is rather trivial if the marginal distribution of the points x -coordinates is perfectly uniform (zero standard deviation) considering a histogram with C bins, and the marginal distribution of the y -coordinates is also perfectly uniform but considering a histogram with R bins. If such distribution holds, the points are very close to the center of individual grid cells, and the displacement to assign them is minimum (P5). In practice, however, this only holds for overlap-free layouts (or close to that).

Based on this observation, we devise a new algorithm that recursively bisects \mathcal{C} into non-overlapping partitions until the obtained partitions individually present perfectly marginal uniform distributions. Then, each partition is assigned to a (sub)grid derived from \mathcal{G} . The spatial partitioning strategy we use is similar to k-d trees [3], but instead of only considering point positions to segment the space, it incorporates the grid restriction and translates points to grid cells. Given such constraint, we have $R - 1$ different options for horizontal splits and $C - 1$ for vertical splits for the first bisection. So the question is how to select the best bisection, or the sequence of horizontal and vertical bisections, that produces the largest partitions with uniform marginal distributions. This is an impractical combinatorial problem to solve. Instead, we split \mathcal{C} approximately in half in the direction (vertical or horizontal) with more rows or columns. In this way, without any expensive test, we increase our probability of getting the largest partitions with marginal uniform distributions – if the number of points in one partition decreases, this probability increases. However, it reduces such a probability for the other partition. Therefore half is a natural trade-off.

In our process, if $R > C$, we split \mathcal{C} horizontally, obtaining two partitions $\mathcal{C} = \mathcal{C}_1 \cup \mathcal{C}_2$, so that the top partition \mathcal{C}_1 contains enough points to fill (approximately) half of the target grid, that is, $|\mathcal{C}_1| = \lceil R/2 \rceil \times C$. Otherwise, we split \mathcal{C} vertically, so that the left partition \mathcal{C}_1 contains enough points to fill (approximately) half of the target grid, that is, $|\mathcal{C}_1| = R \times \lceil C/2 \rceil$. This bisecting process is recursively applied to the

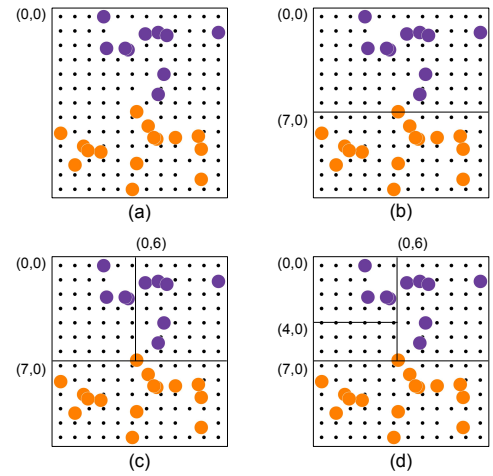


Fig. 3. Process of assigning points to grid cells. In this example, a scatterplot with 156 “dummy” and original points (a) is assigned to a grid with 13 rows and 12 columns. Starting from a horizontal bisection (b), the scatterplot is recursively split until each partition contains only one point, resulting in the grid cell indexes.

resulting partitions until obtaining partitions with marginal uniform distribution. This bisecting process results in the minimum displacement for partitions with perfect uniform marginal distributions. Therefore, instead of penalizing our approach’s running time by adding the uniform constraint test, we execute the bisecting process until each partition contains only one point, rendering a much faster and simpler process to implement.

The last piece to discuss is how to calculate the grid cell indexes (positions) to which the points in \mathcal{C} are assigned. Without loss of generality, if the first bisection vertically splits $\mathcal{C} = \mathcal{C}_1 \cup \mathcal{C}_2$, so that $|\mathcal{C}_1| = R \times \lceil C/2 \rceil$, by construction, the index of the most-left column to which points in \mathcal{C}_1 will be assigned is 0, and the index of the most-left column to which points in \mathcal{C}_2 will be assigned is $\lceil C/2 \rceil$. Similarly, for a horizontal split, the index of the most-top row to which points in \mathcal{C}_1 will be assigned is 0, and the index of the most-top row to which points in \mathcal{C}_2 will be assigned is $\lceil R/2 \rceil$. In the general case, when an input partition is assigned to a grid with R' rows and S' columns, if (i, j) is the index of the top-left corner cell of the input grid, the index of the top-left corner cell to which points in \mathcal{C}_1 will be assigned is (i, j) , and the index of the top-left corner cell to which points in \mathcal{C}_2 will be

assigned is $(i + \lceil R'/2 \rceil, j)$ for a horizontal cut, and $(i, j + \lceil C'/2 \rceil)$ for a vertical cut. If the input partition has only one point, (i, j) is the cell index to which the single point is assigned.

Fig. 3 outlines this process. In this example, a scatterplot with 25 original points and 131 “dummy” points (small black dots) is assigned to a grid with $R = 13$ rows and $C = 12$ columns. To start this process, we set the top-left corner cell index to $(0, 0)$ (Fig. 3(a)). Since the input grid has more rows than columns, the first bisection is horizontal (Fig. 3(b)). The resulting top partition contains (approximately) half of the rows (7), and the top-left corner cell of the resulting (sub)grid receives the index $(0, 0)$. The bottom partition contains the remaining rows (6), and the top-left corner cell receives the index $(7, 0)$. Next, the top partition is bisected (Fig. 3(c)). Since the (sub)grid resulting from this partition has more columns than rows, it is vertically split. Again, each resulting partition receives half of the columns (6). The top-left corner cell of the resulting grid from the left partition receives the index $(0, 0)$, whereas the top-left corner cell of the resulting grid from the right partition receives the index $(0, 6)$. This partitioning process is then recursively applied to the resulting partitions (Fig. 3(d)) until each partition contains only one point.

Algorithm 2 puts all these pieces together. Function $\text{SPLIT}_y(\mathcal{C}, K)$ performs the horizontal bisection. In this process, \mathcal{C} is sorted according to the y -coordinates (\mathcal{C} is viewed as a list). The first K points are assigned to \mathcal{C}_1 and the remaining to \mathcal{C}_2 . The function $\text{SPLIT}_x(\mathcal{C}, K)$ performs the vertical bisection using the same process, but sorting \mathcal{C} according to the x -coordinates. Notice that, from an implementation perspective, we use a pre-sorting strategy [7] so that the x - and y -coordinates are only sorted once. Although we have discussed our process as a grid index assignment, the depicted algorithm already transforms such indexes into coordinates multiplying the indexes by the maximum glyphs bounding box (w_{max}, h_{max}) .

Algorithm 2 Assigning points to grid cell positions.

Input:

$\mathcal{C} = \mathcal{P} \cup \mathcal{D}$ \triangleright Scatterplot with “dummy” and original points
 R, C \triangleright Grid dimensions (rows and columns)
 w_{max}, h_{max} \triangleright Max glyph width/height in \mathcal{P}

Output:

$\mathcal{P}' = \{p'_1, \dots, p'_N\}$ \triangleright Transformed points

function $\text{DGRID}(\mathcal{C}, (R, C))$
 $\text{DGRID_AUX}(\mathcal{C}, (R, C), (0, 0))$
return \mathcal{P}'
end function

function $\text{DGRID_AUX}(\mathcal{C}, (R, C), (i, j))$
if $\mathcal{C} \neq \emptyset$ **then**
 if $|\mathcal{C}| = 1$ **then** $\triangleright \mathcal{C}$ has one point
 if $c \in \mathcal{C}$ is an original point **then**
 $\mathcal{P}' \leftarrow \mathcal{P}' \cup (j \times w_{max}, i \times h_{max})$
 end if
 else
 if $R > C$ **then**
 $\mathcal{C}_1, \mathcal{C}_2 \leftarrow \text{SPLIT}_y(\mathcal{C}, \min(|\mathcal{C}|, \lceil R/2 \rceil \times C))$
 $\text{DGRID_AUX}(\mathcal{C}_1, (\lceil R/2 \rceil, C), (i, j))$
 $\text{DGRID_AUX}(\mathcal{C}_2, (R - \lceil R/2 \rceil, C), (i + \lceil R/2 \rceil, j))$
 else
 $\mathcal{C}_1, \mathcal{C}_2 \leftarrow \text{SPLIT}_x(\mathcal{C}, \min(|\mathcal{C}|, R \times \lceil C/2 \rceil))$
 $\text{DGRID_AUX}(\mathcal{C}_1, (R, \lceil C/2 \rceil), (i, j))$
 $\text{DGRID_AUX}(\mathcal{C}_2, (R, C - \lceil C/2 \rceil), (i, j + \lceil C/2 \rceil))$
 end if
 end if
end if
end function

Notice that, since each original and “dummy” point is assigned to an individual cell, and we have the same number of points and cells, the result is a complete overlap-free representation (**P1**).

3.2.3 Computational Complexity

To set DGrid’s computational complexity, we first split the suggested process into two major phases, “dummy” points creation and grid assignment. Considering $T = R \times C > N$ the total number of grid cells, the complexity of creating the “dummy” points is $O(T \log T)$ if a nearest neighbor data structure is used to find the nearest neighbors, such as a k -d tree [3], and a $O(n \log n)$ sorting algorithm is applied to define the final list of points (FILTER() function). For the second phase, if an $O(n \log n)$ algorithm is also used to sort the points’ x - and y -coordinates, its computational complexity is $O(T \log T)$. Assuming that the original scatterplot occupies a finite area and that the ratio between this area and the summation of all glyphs area is bounded by a small constant (see Eq. (10)), DGrid’s overall complexity is $O(N \log N)$.

4 RESULTS

In this section, we present different examples to highlight the advantages of using an overlap-free layout if compared to traditional DR layouts, quantitatively evaluate and compare DGrid against the state-of-the-art, and finish with a user evaluation to measure subjective elements that are not possible to capture through quality metrics.

4.1 Use-Cases

To illustrate the benefits of using overlap-free layouts produced by DGrid, we present different examples in this section. The first, presented in Fig. 1, shows a t-SNE [57] projection and layouts produced using DGrid varying the area allocated to the visual space. In this example, the dataset is the *UCI ML Breast Cancer Wisconsin* [13] composed of 569 samples of *malignant* and *benign* cancer imaging diagnosis.

In the original layout produced by t-SNE (Fig 1(a)), some of the malignant samples (in red) are occluded by benign samples (in gray) since the dataset is ordered by label, and the red points are rendered before the gray points. When DGrid is applied, these points become visible. Observe the now visible red point, a malignant sample close to the center of gray points (Fig 1(b)), completely occluded on the original layout. This outlier has practically the same feature values as some benign cancer samples and is very different from most malignant ones. By observing only the original layout, this fact could probably be ignored. Despite the benefits, since the space allocated to the overlap-free layout is the same as the original layout ($\Delta = 1.0$), the frontiers between groups and sub-groups are blurred. So, fine differences that could be spotted in different sub-groups are lost. This problem can be mitigated by increasing the visual area, in other words, by reducing glyphs’ sizes (Fig 1(c)-(f)). When the area is 50% larger than the original layout ($\Delta = 1.5$), those frontiers become noticeable, and the separation between groups and sub-groups emerges. When the area is doubled ($\Delta = 2.0$), most of the structure of the original layout is captured. However, glyphs become noticeably smaller, and user participation in deciding the correct balance between details and glyph sizes becomes necessary. Once DGrid is very fast, with interactive rates for datasets with a few thousand instances, on-the-fly experimentation during data analysis is possible.

Beyond the usual color-coded circular glyphs, the benefits of using richer glyphs have been discussed in the literature as a means to join the quick overview afforded by DR layouts with the ability of glyph-based visualizations to convey information about the original data dimensions [28]. In these cases, the benefit of using overlap-free layouts is even more evident. Fig. 4 presents such an example where *starglyphs* [20] are used to encode the original multidimensional information. This example uses the *World Happiness Report 2019* [26] dataset¹. This dataset presents a ranking of 156 countries based on a score representing how happy their citizens perceive themselves and other six variables to support the explanation of the happiness variation across countries, including GDP per capita, social support, healthy life expectancy, freedom to make life choices, generosity, and perception of corruption.

We project this dataset using the UMAP [36] technique considering these six variables. Fig. 4(a) presents the original overlapped layout (a

¹<https://www.kaggle.com/unsdsn/world-happiness>

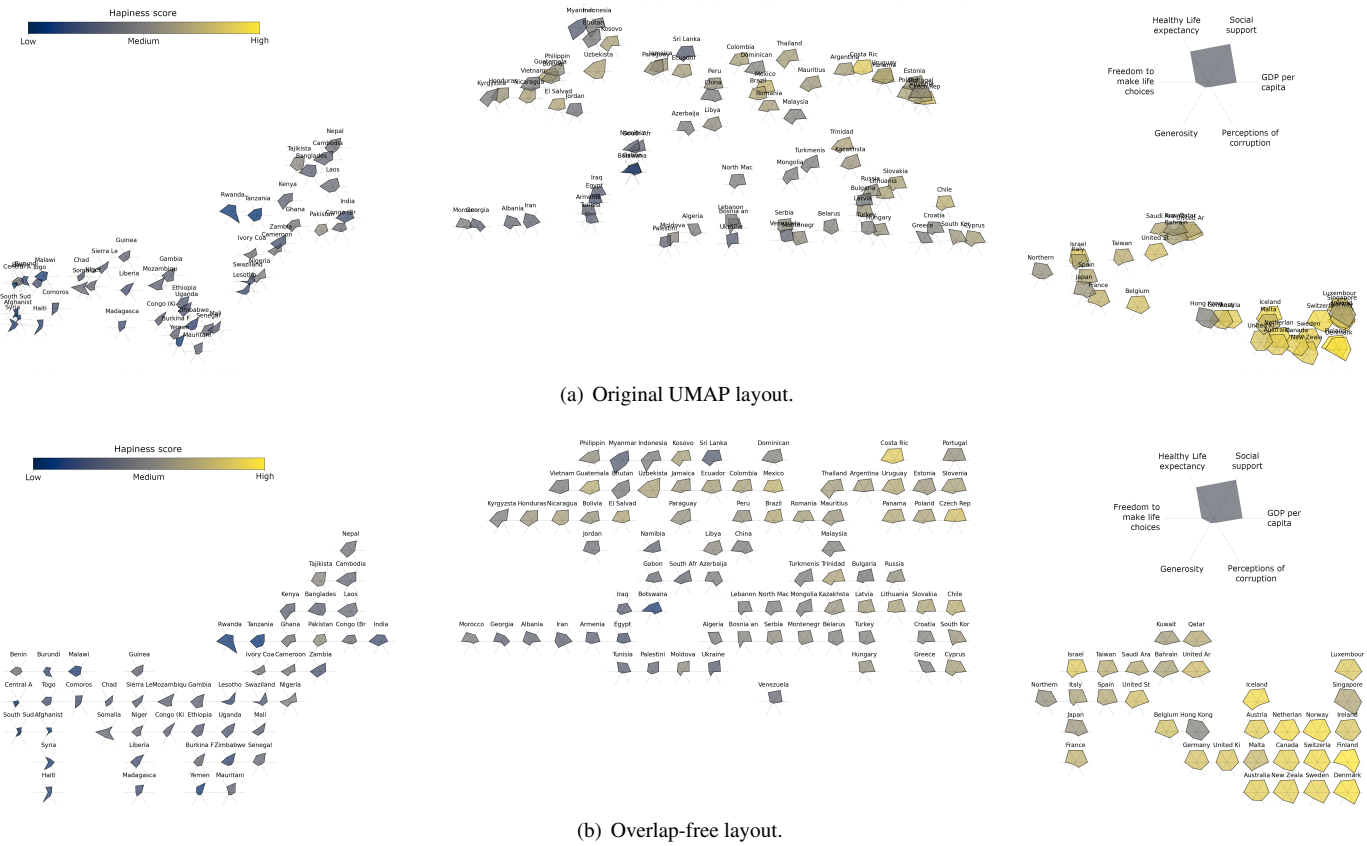


Fig. 4. Original and DGrid overlap-free layouts of a projection from the World Happiness Report 2019 data [26]. Glyphs encode the perceived happiness as color, and the other six variables are mapped to a starglyph. Even for a small dataset, overlaps affect intra-group analysis and a detailed view of the individual instances in the original layout (a). On the overlap-free representation, intra-group analysis is enhanced, allowing detailed examination of individual instances and existing patterns, helping users take advantage of DR layouts combined with richer glyphs.

high-resolution version of this image is included in the supplemental material). Glyphs encode the happiness score as color, and the country names are written on the top of each glyph. In this layout, three different groups of countries are noticeable, one with high happiness scores, another with low scores, and a transition group composed of countries in between these two. Only a few glyphs are “readable”. Most are not easy to understand without an auxiliary strategy (e.g., zoom). Here we use transparency, a usual solution when simple glyphs are used, to mitigate some overlap problems, but it does not help much. In this example, it is difficult to extract any other information beyond group formation, even for this considerably small dataset.

The same projection after removing overlaps with DGrid is presented in Fig. 4. Even after reducing empty space, the three different groups are still noticeable, and many other details are visible. In each one of the groups, the general magnitude of the variables follows the same pattern, although it is possible to see that this is not uniform (we use Euclidean distance, so this is expected). And when checking individual countries, some interesting findings can be derived. For example, generosity varies without following the happiness pattern. Finland (bottom-right), for instance, has a low level of perceived generosity but a high level of happiness, while Haiti (bottom-left) presents the opposite behavior. However, we also have Iceland with high generosity and high happiness and Senegal with low generosity and low happiness. A different observation can be made considering GDP per capita, where usually the richer countries present more significant happiness scores. Of course, with some exceptions, like Costa Rica, a not rich country with high happiness, and Hong Kong, a rich but with a low score. Many other findings can be extracted from this layout, made possible by using more informative glyphs and removing overlaps, leveraging DR layouts to be valuable beyond clustering/segmentation tasks, allowing

the detailed inspection of individual data instances.

Our last example shows the benefit of using DGrid to process larger datasets, presenting how it can improve Convolutional Neural Networks (CNN) analysis based on DR layouts. In this example, we project the test set with 10,000 images from the Fashion MNIST [62] dataset using the dense layer as features. The network we use has two convolutional layers, followed by a dense layer with 128 neurons, followed by a soft-max layer with 10 neurons. Fig. 5 shows the original UMAP layout on the left and the DGrid overlap-free on the right. The circles representing the data instances are color-coded according to the ground truth labels of the images, with red points representing the CNN misclassifications.

Some interesting global insights (inter-group) can be derived from these visual representations. For instance, this particular classifier is very precise for “trousers” (light purple) and “bags” (light green) since those groups are clearly separated from the others. However, it has difficulties distinguishing between “coats” (green), “shirts” (gray), and “pullovers” (blue), given the high incidence of error and the unclear frontiers between these groups. Also, this classifier considers “sandals” (pink), “sneakers” (pink), and “ankle bots” (yellow) similar; however, it successfully differentiates between them, with most of the errors in the frontiers between groups.

Although such observations can be made using both the original or the over-free layouts, the magnitude of the error is arguably more apparent in the overlap-free version, and rendering order issues are avoided. However, the advantages of an overlap-free layout emerge when class-outlier analysis (intra-group) is executed. The class-outlier analysis is an essential task in classification models and focuses on assessing instances of a given class (colors in this example) inside a homogenous group of another class [51]. For this analysis, notice the two highlighted clusters in the original DR layout. Fig. 5(A) shows a

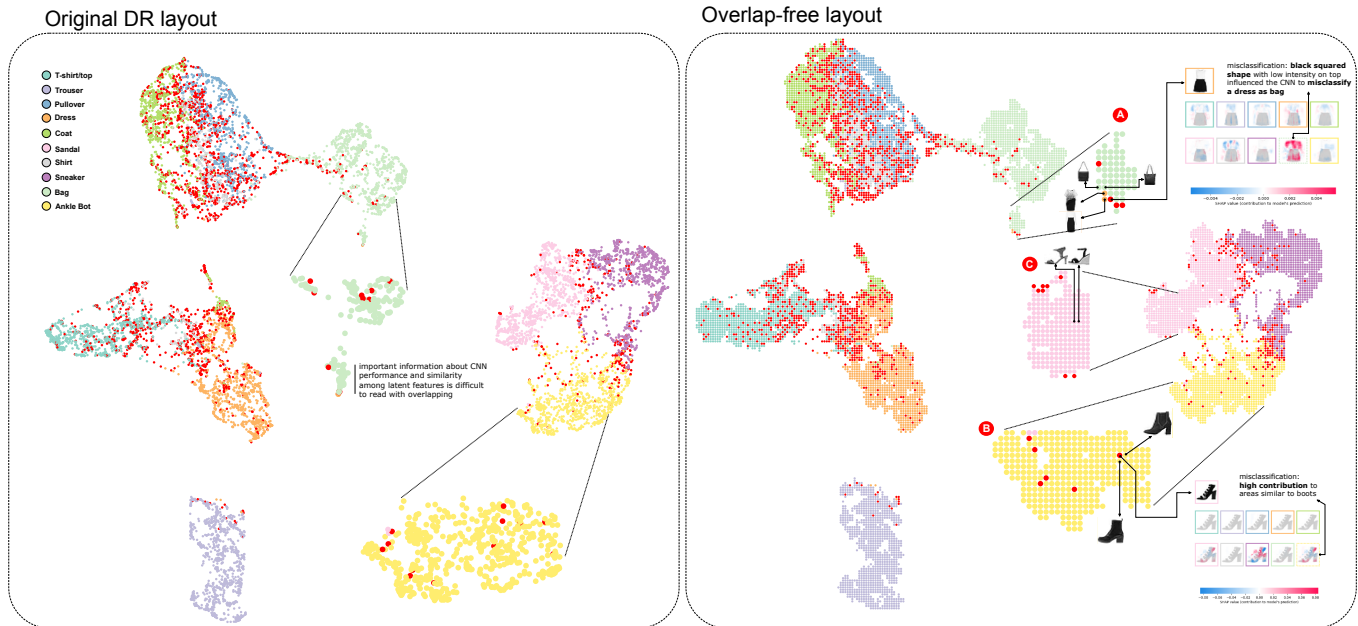


Fig. 5. Using dimensionality reduction and DGrid to analyze CNN results. The original layout is produced using UMAP, and the instances are colored according to ground truth (A). After applying DGrid to remove overlaps, the general appearance is maintained, but class-outliers are easier to spot (B). One group is zoom in for analysis, and images are used as glyphs, allowing the visualization of intra-group patterns (C). To further investigate misclassifications, SHAP is used to show which part of the images contributes to the classification mistakes (D).

zoom-in of a subcluster of “bags” images (in green). In the overlap-free representation, it is possible to see some class-outlier examples and misclassifications that are hidden in the original layout. In this sub-cluster, two instances from the “dress” class (in orange) are far away from their ground-truth cluster, indicating that, although the CNN model was able to classify them correctly, these images are very similar to some “bags”. This is confirmed by checking the original images, where it is possible to verify the similarity between these two dresses and nearby bags. Also, notice the close misclassified instance (in red), a dress classified as a bag. To help understand why the classifier has confused this sample, we use SHAP [32] to explain which part of the image contributed more to the final classification. It is possible to notice that the intensity distribution makes it look like a purse and that the predicted class (“Bag”) presents a high contribution (reddish colors) to the full extent of the image, indicating that this CNN may have problems when classifying this particular type of dress.

Finally, Fig. 5(B) highlights another example that DGrid makes it easier to understand and look for class-outliers. In this case, we select a “sandal” misclassified as an “ankle boot” placed in the middle of the well-defined group of “ankle boots” (yellow). In other words, it is a sandal image very similar to ankle boots from the classifier perspective. SHAP indicates the high intensity and the heels contribute to the misclassification. Nearby ankle boot images are shown for comparison, and in Fig. 5(C) two samples from the “Sandal” class are presented for illustration. It is interesting to notice that, when looking for (real) similar images on the Internet, it is possible to find the definition of “Gladiator Strappy Ankle Boots Heels Sandals.” So a challenging image to even define its ground-truth.

4.2 Evaluation and Comparison

For the quantitative evaluation, we compare DGrid against ReArrange, PFS², VPSC, RWordle-L, RWordle-C, ProjSnippet, and PRISM techniques (see Sec. 2). In this comparison, we use the 7 different quality metrics defined in Sec. 3.1 aiming at assessing the readability and structure preservation of the resulting overlap-free scatterplots.

For the tests, we generate 1,000 different scatterplots varying the sizes between 500 and 1,000 points, the densities, that is, the ratio between scatterplots and glyphs’ area (see Eq.(10)) in {3, 5, 7, 9, 11}, the aspect-ratios between [1, 4], and the number of groups in {1, 2, 3, 4, 5}.

To generate such groups, points coordinates are generated using different Gaussian distributions allowing to control the density of each group and the level of overlap among groups. We prefer to use synthetic scatterplots since this allows us to better control the experiments, producing layouts with varying aspects and helping to uncover the reasons for the attained results. All the results were generated in an Intel(R) Core(TM) i7-8700 CPU @ 3.20 GHz, 32 GB RAM, Ubuntu 64 bits, NVIDIA GeForce GTX 1660 Ti 22 GB. The techniques were implemented in Java. For the ReArrange, RWordle-C, and RWordle-L, we used the authors’ original codes, and we implemented the others. We also implemented DGrid in Python, and the code with all the examples presented in the previous section is publicly available².

Our analysis is presented in Figs. 6 and 7. Fig. 6 presents boxplots summarizing the results of each technique considering the different metrics. Fig. 7 presents heatmaps with correlations between these metrics and the original scatterplots densities (Eq. 10) and overlap coefficients (Eq. 1). We use this correlation analysis to understand, per technique, how the different characteristics of the original scatterplots may affect the quality of the produced overlap-free layouts. In the heatmaps, we only show cells with statistical significance ($\rho < 0.01$).

Interestingly, PFS², VPSC, ProjSnippet, and PRISM were not able to entirely remove overlaps (Fig. 6). The problems of ProjSnippet and PRISM have roots in the employed optimization process and numerical stability. We tried to use gradient clipping to alleviate issues with gradient exploding, but with limited success. For the PFS² and VPSC, we cannot fully understand the causes, but we know that the resulting overlap is positively correlated with the original scatterplots overlap (Fig. 7). That is, as the original overlap increases, the final overlap also increases. Notice that this is also true for the ProjSnippet and PRISM, with a fascinating negative correlation for ProjSnippet (no clues why). For both techniques, the negative result in overlap removal is also correlated with the original scatterplots’ density, meaning that these techniques do not work properly when the amount of visual area that is needed to remove the overlaps approaches the scatterplot total area. DGrid, ReArrange, RWordle-L, and RWordle-C, completely removed the overlaps in all scenarios.

In terms of aspect-ratio preservation (Fig. 6), DGrid is the only

²<https://github.com/fpaulovich/dimensionality-reduction>

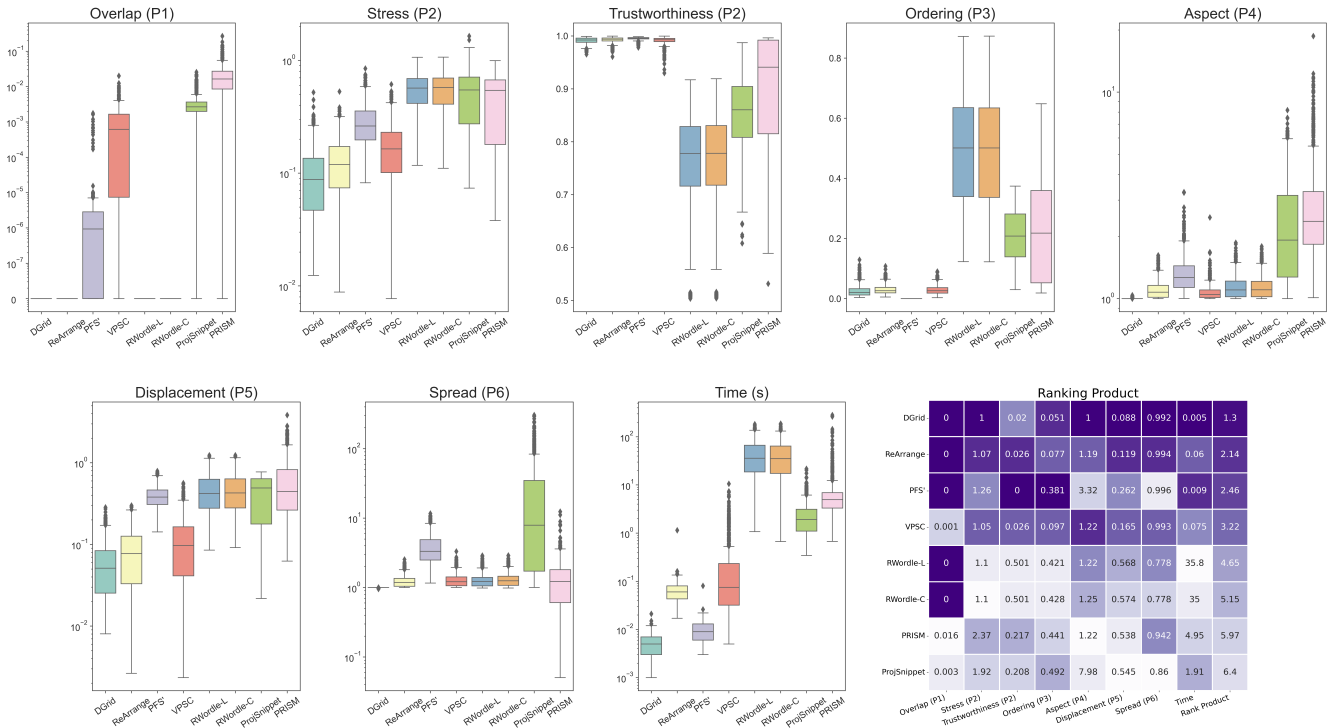


Fig. 6. Boxplots summarizing the results of each technique considering the different metrics defined in Sec. 3.1 and the running time. A Ranking Product matrix is also presented, aggregating all the results to rank the techniques according to their median results. The cells' values are the median, and the darker the cell, the better the ranking position. Considering the combination of all these metrics, DGrid is the top-ranked technique.

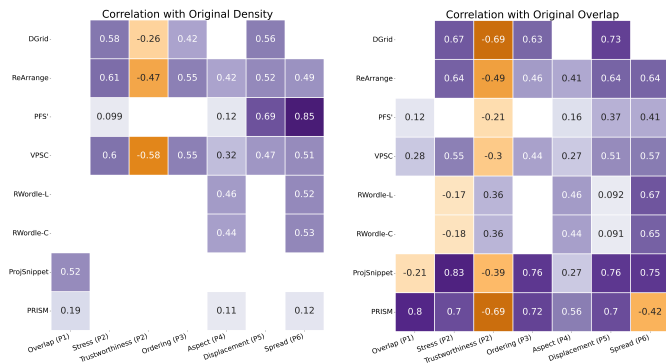


Fig. 7. Correlation heatmaps showing how the densities and overlap coefficients of original scatterplots may influence, per technique, the quality of the produced layouts. The missing cells are correlations without statistical significance.

technique to reach a nearly optimum result, meaning that it is the only technique that can preserve original scatterplots' global shapes while PFS', ProjSnippet, and PRISM present the most significant deformations. Checking the heatmaps (Fig. 7), it is possible to see that DGrid is also the only technique that does not present statistically significant correlation between original scatterplots overlap and density and the aspect-ratio preservation of the produced overlap-free layouts. The others present positive correlation, indicating that overlap and density may negatively affect aspect-ratio, resulting in distorted layouts. Similar results are presented for the spread. DGrid offers a nearly perfect spread, meaning it well preserves original glyphs sizes. PFS' and ProjSnippet present the most significant spread, and PRISM often reduces the scatterplot area's size. For most techniques, the spread is correlated to original density and overlap (since there is no variance

on DGrid results, there is no correlation). This is not surprising since we intentionally preserve the original aspect-ratio and control the displacement by defining our grid dimensions according to the original scatterplot and using it as a constraint to moving points. The other techniques do not set these as hard restrictions, probably not to affect other metrics. Notice that, even with gradient clipping, PRISM could not create bounded overlap-free scatterplots for two scenarios. So we removed them from PRISM analysis.

Displacement and stress present similar results. DGrid renders the best result, closely followed by ReArrange and VPSC. PFS' presents intermediate results and the others are on the same level of low distance preservation and high displacement. Therefore, DGrid, ReArrange, and VPSC maintain the original scatterplot's general appearance, with low displacement and good global preservation of original distances. Locally, DGrid, ReArrange, PFS', and VPSC present practically the same results regarding trustworthiness, with PFS' attaining the best result. Not only do these techniques present the best results, but also the deviation is minimal. This indicates that neighborhoods are reliable, a fundamental characteristic since several analytical tasks executed using DR scatterplots are based on neighborhood analysis. Notice that it is necessary to establish the neighborhood size to calculate trustworthiness. Here we use the common heuristic of setting it to 5% of the scatterplot size.

For the last metric, orthogonal ordering, PFS' renders the perfect result, with DGrid, ReArrange, and VPSC close by. These techniques have the lowest impact on the user's mental map, meaning that if the user puts side-by-side the original and the transformed layout and focuses the analysis on one point, what is at the top/bottom, left/right of that point is preserved. However, for most techniques, there is a cost for that, which is an increased spread. ReArrange and VPSC increase the scatterplot sizes by 20% while the PFS' increases more than 330%. DGrid ensures good orthogonal ordering without incurring in expanding the scatterplot area, preserving the perceived glyphs' sizes.

In terms of running times, even though the datasets are small, two

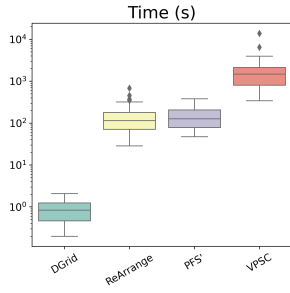


Fig. 8. Boxplot summarizing the results considering larger datasets ($50k \sim 100K$ instances). Compared to the four fastest techniques, DGrid is two or three orders of magnitude faster.

groups of techniques can be observed: one containing techniques that run under a second; and another composed of methods that need more (for some, much more) than that. DGrid is the fastest technique, with ReArrange, PFS' and VPSC practically presenting the same execution time (the difference is in milliseconds). To show the real differences between these four faster techniques, we create 120 datasets following the same procedure explained before, but with sizes varying between 50,000 and 100,000. Fig. 8 presents the boxplot summarizing the results. DGrid (median=0.83s) is at least two orders of magnitude faster than the ReArrange (median=114.89s) and PFS' (median=126.91s) and three orders faster than VPSC (median=1,471.35s).

Finally, we calculate the rank product [6] using all metrics and running-time (for the small datasets) to summarize these results. Rank product is a non-parametric statistical method used in biology to combine different ranks and define a general rank. If $r_{t,i}$ denotes the rank position of technique t in the i^{th} metric, the final rank of t considering K different metrics is calculated as $(\prod_i^K r_{t,i})^{1/K}$. In our case, for each metric, we create a rank based on the techniques' median values (rounding to the 3rd decimal place). Fig. 6 presents a heatmap showing the median results of each technique for each metric, with the cells colored according to the rank position per metric. The darker the color, the best the rank position. DGrid presents the best trade-off between all the techniques and is ranked the first in terms of attending the principles presented in Sec. 3.1. ReArrange and PFS' are in second place, with ReArrange presenting superior results. VPSC appears in the fourth position, RWordle-L in the fifth, RWordle-C and PRISM in the sixth, and ProjSnippet in the last, rendering DGrid a precise and fast approach to remove overlaps.

4.3 User Evaluation

Some characteristics of DGrid, such as the produced layouts' general appearance, are inherently subjective and much harder to capture with objective metrics. For example, the impact of aligning the points into a grid, which interferes with their free distribution but may lead to a more organized look and feel, or how the expansion of highly dense regions hinders user perception of groups and other patterns present on the original scatterplots. To account for these aspects, we executed a user test to evaluate how removing overlap affects user perception of the preservation of patterns and the aesthetics of the produced layouts.

The test consisted of two main parts. In the first, given an original scatterplot (with overlap) and eight possible overlap-free alternatives produced by different techniques, the participant was asked to select a minimum of one and a maximum of three overlap-free layouts that best preserved the general characteristics (patterns) of the original, e.g., global scatterplot format, groups, borders between groups, item positions, and item size. In the second part, given eight overlap-free alternatives produced by different techniques (without the original), the participant was asked to choose the one that is the most aesthetically pleasing and easy to understand (regarding, e.g., separation and boundaries between groups). In both cases, we also ask for optional qualitative feedback regarding the reasons for their choices. Each par-

ticipant assessed 15 sets of scatterplots in the first part (*patterns*) and 10 sets in the second part (*aesthetics*). The scatterplots were anonymized (i.e., the participant did not know which technique generated them), and the presentation order of the eight alternatives was always randomized per set and participant. The test was distributed online via *Google Forms* and was performed by 42 volunteers from various universities in different countries and continents (more information about the participants can be found in the supplemental material).

The results—the distributions of scores for each technique in both parts of the user evaluation—are shown in Fig. 9. In the first part, we compute a score for each technique (per participant) as follows. Every time a technique is selected as one of the best overlap-free alternatives, it receives a score of $1/N_{choices}$, where $N_{choices} \in \{1, 2, 3\}$ is the number of alternatives selected for the same set. Thus, if the participant selected only one alternative, it gets the maximum score of 1 for that specific set; otherwise, it gets a score of either $\frac{1}{2}$ or $\frac{1}{3}$. The final score of that participant's technique is the sum of the scores for all the 15 assessed sets of scatterplots. In the second part, each technique's score (per participant) is simply the number of times it was selected as the most aesthetic-pleasing alternative.

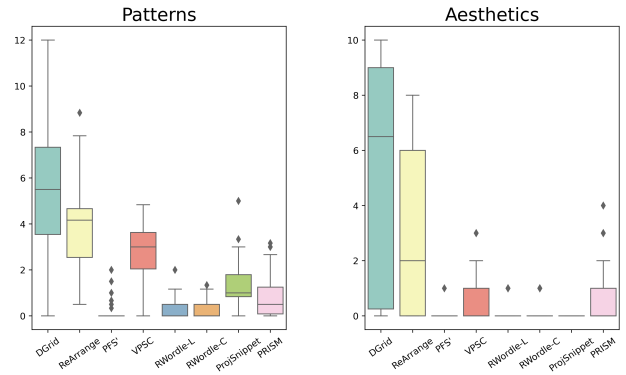


Fig. 9. Results of the user evaluation. DGrid has the highest average scores for both pattern preservation and aesthetics.

DGrid achieves the highest average scores (M) in both parts of the evaluation : ($M = 5.329, SD = 3.060$) for the first (*patterns*), and ($M = 5.166, SD = 4.131$) for the second (*aesthetics*). The second-highest scores come from ReArrange in both cases: ($M = 3.805, SD = 1.797$) for the first part of the test, and ($M = 2.928, SD = 3.063$) for the second. Due to the considerable amount of variability in the results, we further tested DGrid's scores against ReArrange using two one-tailed two-sample t -tests, one for each part. Our null hypotheses are that DGrid's scores are statistically the same as ReArrange's, while our alternative hypotheses are that they are higher (with $\alpha = 0.1$). We chose the t -test due to sample size ($N = 42$) and the approximately-normal shape of the distributions (according to Kolmogorov-Smirnov tests [1]). The results are significant in both cases, with $p = .003351$ for the first part (*patterns*) and $p = .00301$ for the second (*aesthetics*). Thus, we rejected both null hypotheses in favor of the alternative ones.

Finally, we also ask for optional qualitative feedback regarding the reasons for participants' choices when selecting layouts considering best pattern preservation and aesthetics. The main explanations for choosing DGrid include: "less cluttered, boundaries/groups are easy to see, the overall layout looks more stable, labeled points that are placed within other groups (other color) are easy to see", "more compact, less noisy; visualization transformation already does the work that my brain would to identify and emphasize the clusters", and "...the highly ordered displays were easiest to understand and retained information more correctly."; indicating potential benefits of having more organized layouts compared to the original noise/cluttered and other overlap-free representations.

5 DISCUSSIONS AND LIMITATIONS

Design considerations. In our solution for assigning points to a grid (Algorithm 2), the bisecting process uses a simple heuristic to partition the points, splitting them into sub-partitions with similar sizes. As discussed (Sec. 3.2.2), we split in halves since, without any expensive test, we increase the probability of getting the largest partitions with the desired distribution. We have also tested creating partitions with different sizes, but the results were not statistically different. One alternative to improve could be to use a strategy to find the best (orthogonal) partitioning, for instance, using the Jenks’ Natural Break [27]. The Natural Break is a clustering approach that partitions univariate datasets to reduce the variance within-cluster and maximize the variance between clusters. We also tested with that, and the marginal improvement does not justify the increase in complexity and running time. We input two main reasons for this result. First, considering a bisection to produce a (sub)grid with R rows and C columns, we have only $R - 1$ possible horizontal cuts and $C - 1$ possible vertical cuts. So, there is not much room for defining the best partition. Second, since the “dummy” points are distributed following the grid cells, the regions of empty spaces already present perfect uniform marginal distributions, so a different splitting does not change the outcome considerably for scatterplots containing empty spaces.

Another design consideration is why not fix the “dummy” points and move only the original points? Although a reasonable idea, fixing “dummy” points do not work in practice. Since the process of creating such points does not guarantee that the number of not occupied cells close to a high-density region is equal to the number of original points in that region, the original points can be drastically displaced if the “dummy” points do not move.

Space constraints. Although an effective solution to declutter scatterplot layouts, overlap removal may not be the best option in some cases and for some tasks. Firstly, removing overlaps affects distribution detection tasks. This is true for all techniques that limit the visual area to keep glyphs at a readable size. A simple solution could be to show the original and the overlap-free scatterplots side-by-side. In this case, a precise technique, such as DGrid or ReArrange, is mandatory, so the user’s mental map is preserved between visualizations. Secondly, the visual area where the overlap-free scatterplot is rendered needs to allow the removal. It is possible to remove overlaps only if the proportion between the available space and total glyphs area is larger than one (see Eq. 10). Indeed, if this proportion is not significant and the original scatterplot presents high-density regions, the produced scatterplot will merge groups and fine-grained groups will be blended, impacting class separation tasks [40]; an issue affecting all overlap removal techniques. One solution is to increase the available space, in our case, increasing Δ , but incurring reduced glyphs’ size if the display space is not increased. This is especially problematic for large datasets, where Δ may need to be too big to accommodate all points and empty spaces. In this situation, a sampling technique [63] may be a better choice to help declutter the visual representation. In fact, the choice between overlap removal or sampling should be based on the analytical task at hand and the data set size. Sampling may be a better choice if the goal is to have an overview of a (large) dataset in terms of group formation. However, if visual space allows and beyond groups, the analytical task also involves inspecting individual instances, overlap removal may be better suitable. One idea to take advantage of both concepts is to use sampling and overlap removal together, for instance, aggregating points before removing the overlaps. This involves several practical challenges, so we leave this idea for future work.

Glyph’s shape and dimension. DGrid allocates the same layout area to each glyph (grid cells). Although glyphs’ dimensions can vary inside that area, if they are too discrepant, unnecessary space will be added to the overlap-free layout. Similarly, if the shapes of the glyphs deviate too much from the rectangular form (they can indeed assume any form), unnecessary spaces between glyphs may also be created. For circular (like pie-charts), diamond, or hexagon-shaped glyphs, DGrid can be easily adapted to address this issue by horizontally and vertically

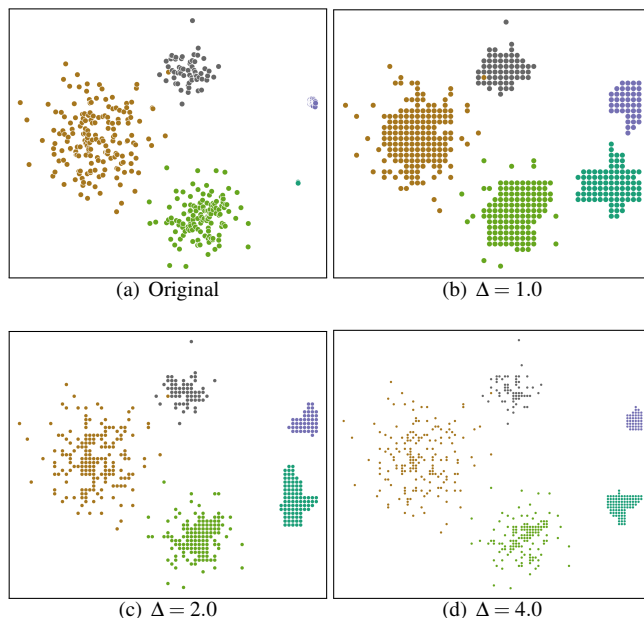


Fig. 10. A corner case for removing overlap. A significant density variation can be observed with two very dense groups (purple and dark green). Although overlap can be fully removed and some distortions can be reduced by increasing Δ , some are still inevitable.

translating the grid rows by small fractions of the glyphs’ maximum width and height. Although an effective solution, this changes the scatterplot aspect-ratio (violating P4), so a better solution would be to design an assignment process that considers different partitions of the space. We leave this as future work as well. In summary, although the resulting grid alignment showed beneficial, bringing some organization to the visualization, other solutions for removing overlap are preferable if glyphs with significantly varying shapes and dimensions are required.

Distortions and evaluation. Overlap removal in scatterplots is a well-documented strategy [52, 53], with different added benefits given the more readable visual representations it generates [38]. However, it introduces distortions in the produced representations. For example, the scatterplot of Fig. 10(a) is an example where it is inevitable to add distortions in the overlap-free layout due to density variation and the presence of very high-dense groups of points (purple and dark green). For DGrid, since we use orthogonal partitioning in the grid assignment process, these high-dense groups, especially those close to the scatterplot borders, tend to have rectangular sides or shapes. This can be mitigated, up to an extent, by increasing Δ (Fig. 10(b-d)) but paying the price of reducing the glyphs and potentially creating unreadable layouts.

Finally, although our user test indicates that DGrid, compared to other techniques, presents a good ability to preserve the original patterns (groups, borders between groups, outliers, etc.), the whole concept of overlap removal would benefit from a more extensive evaluation to verify in the wild the real benefits of an overlap-free layout and what are the introduced caveats. This is a very complex evaluation, beyond our scope, but important future work.

6 CONCLUSIONS

In this paper, we proposed *Distance-preserving Grid (DGrid)*, a novel approach for overlap removal of Dimensionality Reduction (DR) layouts. DGrid is a two-step approach that completely removes overlap and maintains the original scatterplot aspect ratio and glyphs’ sizes while preserving distance and neighborhood relationships, an essential feature for DR layouts. The set of comparisons we provide shows that DGrid outperforms the existing state-of-the-art techniques considering different quality metrics and is two to three orders of magnitude faster

than the fastest existing techniques. A user test attests the good results, with most participants selecting DGrid layouts as ones that best preserve original patterns and are aesthetically pleasing. The quality of the produced layouts combined with the low computational cost render DGrid one of the most attractive methods to date, allowing inter-group and class-outlier analyses that are usually challenging in typical DR layouts.

ACKNOWLEDGMENTS

The authors would like to thank all reviewers that dedicated time to this paper. Your comments and feedback were beneficial and indeed led to substantial improvement in the quality and clarity of this manuscript. We acknowledge the support of the Natural Sciences and Engineering Research Council of Canada (NSERC), CAPES-Brazil, and the Emerging Leaders in the Americas Program (ELAP) with the support of the Government of Canada.

REFERENCES

- [1] *Kolmogorov–Smirnov Test*, pp. 283–287. Springer New York, New York, NY, 2008. doi: 10.1007/978-0-387-32833-1_214
- [2] J. A. Anderson and E. Rosenfeld, eds. *Neurocomputing: Foundations of Research*. MIT Press, Cambridge, MA, USA, 1988.
- [3] J. L. Bentley. Multidimensional binary search trees used for associative searching. *Commun. ACM*, 18(9):509–517, Sept. 1975.
- [4] E. Bertini and G. Santucci. Give chance a chance: Modeling density to enhance scatter plot quality through random data sampling. *Information Visualization*, 5:110–95, 2006.
- [5] R. Brath. 3d infovis is here to stay: Deal with it. In *2014 IEEE VIS International Workshop on 3DVis (3DVis)*, pp. 25–31, 2014. doi: 10.1109/3DVis.2014.7160096
- [6] R. Breitling, P. Armengaud, A. Amtmann, and P. Herzyk. Rank products: a simple, yet powerful, new method to detect differentially regulated genes in replicated microarray experiments. *FEBS Letters*, 573(1-3):83–92, 2004. doi: 10.1016/j.febslet.2004.07.055
- [7] R. A. Brown. Building a balanced k -d tree in $o(kn \log n)$ time. *Journal of Computer Graphics Techniques (JCGT)*, 4(1):50–68, March 2015.
- [8] N. Cao, D. Gotz, J. Sun, and H. Qu. Dicon: Interactive visual analysis of multidimensional clusters. *IEEE Transactions on Visualization and Computer Graphics*, 17(12):2581–2590, 2011. doi: 10.1109/TVCG.2011.188
- [9] D. B. Carr, R. J. Littlefield, W. L. Nicholson, and J. S. Littlefield. Scatterplot matrix techniques for large n . *Journal of the American Statistical Association*, 82(398):424–436, 1987. doi: 10.1080/01621459.1987.10478445
- [10] F. Chen, L. Piccinini, P. Poncelet, and A. Sallaberry. Node overlap removal algorithms: an extended comparative study. *Journal of Graph Algorithms and Applications*, 24(4):683–706, 2020. doi: 10.7155/jgaa.00532
- [11] F. Chen, L. Piccinini, P. Poncelet, and A. Sallaberry. Node overlap removal algorithms: an extended comparative study. *Journal of Graph Algorithms and Applications*, 24(4):683–706, 2020. doi: 10.7155/jgaa.00532
- [12] X. Chen, T. Ge, J. Zhang, B. Chen, C.-W. Fu, O. Deussen, and Y. Wang. A recursive subdivision technique for sampling multi-class scatterplots. *IEEE Transactions on Visualization and Computer Graphics*, 26(1):729–738, 2020. doi: 10.1109/TVCG.2019.2934541
- [13] D. Dua and C. Graff. UCI machine learning repository, 2017.
- [14] F. S. L. G. Duarte, F. Sikansi, F. M. Fatore, S. G. Fadel, and F. V. Paulovich. Nmap: A novel neighborhood preservation space-filling algorithm. *IEEE Transactions on Visualization and Computer Graphics*, 20(12):2063–2071, 2014. doi: 10.1109/TVCG.2014.2346276
- [15] T. Dwyer, K. Marriott, and P. J. Stuckey. Fast node overlap removal. In P. Healy and N. S. Nikolov, eds., *Graph Drawing*, pp. 153–164. Springer Berlin Heidelberg, Berlin, Heidelberg, 2006.
- [16] D. M. Eler, M. V. Nakazaki, F. V. Paulovich, D. P. Santos, G. de Faria Anderson, M. C. F. de Oliveira, J. B. Neto, and R. Minghim. Visual analysis of image collections. *Vis. Comput.*, 25(10):923–937, 2009. doi: 10.1007/s00371-009-0368-7
- [17] N. Elmquist. Balloonprobe: Reducing occlusion in 3d using interactive space distortion. In *Proceedings of the ACM Symposium on Virtual Reality Software and Technology, VRST ’05*, p. 134–137. Association for Computing Machinery, New York, NY, USA, 2005. doi: 10.1145/1101616.1101643
- [18] D. Eppstein, M. van Kreveld, B. Speckmann, and F. Staals. Improved grid map layout by point set matching. In *2013 IEEE Pacific Visualization Symposium (PacificVis)*, pp. 25–32, 2013. doi: 10.1109/PacificVis.2013.6596124
- [19] O. Fried, S. DiVerdi, M. Halber, E. Sizikova, and A. Finkelstein. Isomatch: Creating informative grid layouts. *Comput. Graph. Forum*, 34(2):155–166, May 2015.
- [20] J. Fuchs, P. Isenberg, A. Bezerianos, F. Fischer, and E. Bertini. The influence of contour on similarity perception of star glyphs. *IEEE Transactions on Visualization and Computer Graphics*, 20(12):2251–2260, 2014. doi: 10.1109/TVCG.2014.2346426
- [21] E. Gansner and Y. Hu. Efficient, proximity-preserving node overlap removal. *J. Graph Algorithms Appl.*, 14:53–74, 2010.
- [22] M. v. Garderen, B. Pampel, A. Nocaj, and U. Brandes. Minimum-Displacement Overlap Removal for Geo-referenced Data Visualization. *Computer Graphics Forum*, 2017. doi: 10.1111/cgf.13199
- [23] E. Gomez-Nieto, W. Casaca, L. G. Nonato, and G. Taubin. Mixed integer optimization for layout arrangement. In *2013 XXVI Conference on Graphics, Patterns and Images*, pp. 115–122, 2013. doi: 10.1109/SIBGRAPI.2013.25
- [24] E. Gomez-Nieto, F. S. Roman, P. Pagliosa, W. Casaca, E. S. Helou, M. C. F. de Oliveira, and L. G. Nonato. Similarity preserving snippet-based visualization of web search results. *IEEE Transactions on Visualization and Computer Graphics*, 20(3):457–470, 2014. doi: 10.1109/TVCG.2013.242
- [25] K. Hayashi, M. Inoue, T. Masuzawa, and H. Fujiwara. A layout adjustment problem for disjoint rectangles preserving orthogonal order. In *Graph Drawing*, 1998.
- [26] J. Helliwell, R. Layard, and J. Sachs. *World Happiness Report 2019*. New York: Sustainable Development Solutions Network, 2019.
- [27] G. F. Jenks. The data model concept in statistical mapping. *International Yearbook of Cartography*, 7:186–190, 1967.
- [28] D. Kammer, M. Keck, T. Gründer, A. Maasch, T. Thom, M. Kleinstüber, and R. Groh. Glyphboard: Visual exploration of high-dimensional data combining glyphs with dimensionality reduction. *IEEE Transactions on Visualization and Computer Graphics*, 26(4):1661–1671, 2020. doi: 10.1109/TVCG.2020.2969060
- [29] J. Kruskal. Multidimensional scaling by optimizing goodness of fit to a nonmetric hypothesis. *Psychometrika*, 29(1):1–27, 1964.
- [30] J. Li, J. Martens, and J. J. van Wijk. A model of symbol size discrimination in scatterplots. In *Proceedings of the 28th International Conference on Human Factors in Computing Systems*, 2010.
- [31] J. Li, J. J. van Wijk, and J. Martens. Evaluation of symbol contrast in scatterplots. In *2009 IEEE Pacific Visualization Symposium*, 2009.
- [32] S. M. Lundberg and S.-I. Lee. A unified approach to interpreting model predictions. In I. Guyon, U. V. Luxburg, S. Bengio, H. Wallach, R. Fergus, S. Vishwanathan, and R. Garnett, eds., *Advances in Neural Information Processing Systems 30*, pp. 4765–4774. Curran Associates, Inc., 2017.
- [33] W. E. Marcilio-Jr, D. M. Eler, R. E. Garcia, and I. R. V. Pola. Evaluation of approaches proposed to avoid overlap of markers in visualizations based on multidimensional projection techniques. *Information Visualization*, 18(4):426–438, 2019. doi: 10.1177/1473871619845093
- [34] A. Mayorga and M. Gleicher. Splatterplots: Overcoming overdraw in scatter plots. *IEEE Transactions on Visualization and Computer Graphics*, 19(9):1526–1538, 2013. doi: 10.1109/TVCG.2013.65
- [35] A. Mayorga and M. Gleicher. Splatterplots: Overcoming overdraw in scatter plots. *IEEE Transactions on Visualization and Computer Graphics*, 19(9):1526–1538, 2013. doi: 10.1109/TVCG.2013.65
- [36] L. McInnes, J. Healy, and J. Melville. Umap: Uniform manifold approximation and projection for dimension reduction, 2020.
- [37] G. McNeill and S. A. Hale. Generating tile maps. *Computer Graphics Forum*, 36(3):435–445, 2017. doi: 10.1111/cgf.13200
- [38] W. Meulemans. Efficient optimal overlap removal: Algorithms and experiments. *Computer Graphics Forum*, 38(3):713–723, 2019. doi: 10.1111/cgf.13722
- [39] W. Meulemans, J. Dykes, A. Slingsby, C. Turkay, and J. Wood. Small multiples with gaps. *IEEE Transactions on Visualization and Computer Graphics*, 23(1):381–390, Jan 2017.
- [40] L. Micallef, G. Palmas, A. Oulasvirta, and T. Weinkauff. Towards perceptual optimization of the visual design of scatterplots. *IEEE Transactions on Visualization and Computer Graphics*, 23(6):1588–1599, 2017. doi: 10.1109/TVCG.2017.2674978
- [41] L. Micallef, G. Palmas, A. Oulasvirta, and T. Weinkauff. Towards perceptual optimization of the visual design of scatterplots. *IEEE Transactions*

- on *Visualization and Computer Graphics*, 2017.
- [42] K. Misue, P. Eades, W. Lai, and K. Sugiyama. Layout adjustment and the mental map. *J. Vis. Lang. Comput.*, 6:183–210, 1995.
- [43] K. Misue, P. Eades, W. Lai, and K. Sugiyama. Layout adjustment and the mental map. *Journal of Visual Languages & Computing*, 6(2):183–210, 1995. doi: 10.1006/jvlc.1995.1010
- [44] L. Nachmanson, A. Nocaj, S. Bereg, L. Zhang, and A. Holroyd. Node overlap removal by growing a tree. In Y. Hu and M. Nöllenburg, eds., *Graph Drawing and Network Visualization*, pp. 33–43. Springer International Publishing, Cham, 2016.
- [45] L. G. Nonato and M. Aupetit. Multidimensional projection for visual analytics: Linking techniques with distortions, tasks, and layout enrichment. *IEEE Transactions on Visualization and Computer Graphics*, 25(8):2650–2673, 2019. doi: 10.1109/TVCG.2018.2846735
- [46] R. Pinho and M. C. F. de Oliveira. Hexboard: Conveying pairwise similarity in an incremental visualization space. In *2009 13th International Conference Information Visualisation*, pp. 32–37, 2009. doi: 10.1109/IV.2009.12
- [47] R. Pinho, M. C. F. de Oliveira, and A. de A. Lopes. Incremental board: A grid-based space for visualizing dynamic data sets. In *Proceedings of the 2009 ACM Symposium on Applied Computing*, p. 1757–1764. Association for Computing Machinery, New York, NY, USA, 2009. doi: 10.1145/1529282.1529679
- [48] N. Quadrianto, L. Song, and A. Smola. Kernelized sorting. *IEEE Transactions on Pattern Analysis and Machine Intelligence*, 32:1809–1821, 2010.
- [49] E. Raisz. The rectangular statistical cartogram. *Geographical Review*, 24:292–296, 1934.
- [50] A. B. Ramos-Guajardo, G. González-Rodríguez, and A. Colubi. Testing the degree of overlap for the expected value of random intervals. *International Journal of Approximate Reasoning*, 119:1–19, 2020. doi: 10.1016/j.ijar.2019.12.012
- [51] P. E. Rauber, A. X. Falcão, and A. C. Telea. Projections as visual aids for classification system design. *Information Visualization*, 17(4):282–305, 2018. doi: 10.1177/1473871617713337
- [52] A. Sarikaya and M. Gleicher. Scatterplots: Tasks, data, and designs. *IEEE Transactions on Visualization and Computer Graphics*, 24(1):402–412, 2018. doi: 10.1109/TVCG.2017.2744184
- [53] M. Sedlmair, T. Munzner, and M. Tory. Empirical guidance on scatterplot and dimension reduction technique choices. *IEEE Transactions on Visualization and Computer Graphics*, 19(12):2634–2643, 2013. doi: 10.1109/TVCG.2013.153
- [54] H. Strobel, M. Spicker, A. Stoffel, D. Keim, and O. Deussen. Rolled-out wordles: A heuristic method for overlap removal of 2d data representatives. *Computer Graphics Forum*, 31, 2012.
- [55] G. Strong and M. Gong. Data organization and visualization using self-sorting map. In *Proceedings of Graphics Interface 2011, GI '11*, p. 199–206, 2011.
- [56] M. Tory, D. Sprague, F. Wu, W. Y. So, and T. Munzner. Spatialization design: Comparing points and landscapes. *IEEE Transactions on Visualization and Computer Graphics*, 13(6):1262–1269, 2007. doi: 10.1109/TVCG.2007.70596
- [57] L. van der Maaten and G. Hinton. Visualizing High-Dimensional Data Using t-SNE. *Journal of Machine Learning Research*, 9:2579–2605, Nov. 2008.
- [58] M. van Kreveld and B. Speckmann. On rectangular cartograms. In S. Albers and T. Radzik, eds., *Algorithms – ESA 2004*, pp. 724–735. Springer Berlin Heidelberg, Berlin, Heidelberg, 2004.
- [59] J. Venna and S. Kaski. Neighborhood preservation in nonlinear projection methods: An experimental study. In G. Dorffner, H. Bischof, and K. Hornik, eds., *Artificial Neural Networks — ICANN 2001*, pp. 485–491. Springer Berlin Heidelberg, Berlin, Heidelberg, 2001.
- [60] J. Wood and J. Dykes. Spatially ordered treemaps. *IEEE Transactions on Visualization and Computer Graphics*, 14(6):1348–1355, 2008. doi: 10.1109/TVCG.2008.165
- [61] J. Wood, J. Dykes, and A. Slingsby. Visualisation of origins, destinations and flows with od maps. *The Cartographic Journal*, 47:117 – 129, 2010.
- [62] H. Xiao, K. Rasul, and R. Vollgraf. Fashion-mnist: a novel image dataset for benchmarking machine learning algorithms. *ArXiv*, abs/1708.07747, 2017.
- [63] J. Yuan, S. Xiang, J. Xia, L. Yu, and S. Liu. Evaluation of sampling methods for scatterplots. *IEEE Transactions on Visualization and Computer Graphics*, 27(02):1720–1730, feb 2021. doi: 10.1109/TVCG.2020.